Received 16 May 2020; revised 22 June 2020; accepted 7 July 2020. Date of publication 14 July 2020; date of current version 4 August 2020.

Digital Object Identifier 10.1109/OJAP.2020.3009185

Techniques for Achieving High Isolation in RF Domain for Simultaneous Transmit and Receive

SATHEESH BOJJA VENKATAKRISHNAN [1] (Member, IEEE), ALEXANDER HOVSEPIAN [1] (Student Member, IEEE), ALEXANDER D. JOHNSON [1] (Student Member, IEEE), TOSHIFUMI NAKATANI [2] (Senior Member, IEEE), ELIAS A. ALWAN [1] (Member, IEEE), AND JOHN L. VOLAKIS [1] (Fellow, IEEE)

[1]Department of Electrical and Computer Engineering, Florida International University, Miami, FL 33174, USA

[2]MaXentric Technologies, LLC, La Jolla, CA 92037, USA

CORRESPONDING AUTHOR: S. B. VENKATAKRISHNAN (e-mail: sbojjave@fiu.edu)

This work was supported in part by the Office of Naval Research under Grant N00014-16-1-2253, and in part by the U.S. Army under Contract W911QX18P0203.

ABSTRACT With the growth of wireless data traffic, additional spectrum is required to meet consumer demands. Consequently, innovative approaches are needed for efficient management of the available limited spectrum. To double the achievable spectral efficiency, a transceiver can be designed to receive and transmit signals simultaneously (STAR) across the same frequency band. However, due to the coupling of the high power transmitted signal into the collocated receiver, the receiver's performance is degraded. For successful STAR realization, the coupled high-power transmit (Tx) signal should be suppressed by 100-120 dB over the entire operational bandwidth. So far, most STAR implementations are narrowband, and not useful for ultra wideband (UWB) communications. In this paper, we present a review of novel approaches employed to achieve improved cancellation across wide bandwidths in RF and propagation domains. Both single and multi-antenna systems are considered. Measurements show an average cancellation of 50 dB using two stages of RF signal cancellation.

INDEX TERMS Antenna, balun, isolation, feed network, simultaneous transmit and receive (STAR).

I. INTRODUCTION

NEXT generation mobile and wireless communication systems (5G and beyond) will require increasingly high data rates to support the growing volume of data exchange and expected integration with Internet of Things (IoT) sensors. Also, due to increased consumer demand, additional but discontinuous frequency bands are likely to be allocated for commercial use [1]–[3]. As a result, only a small percentage of the RF spectrum will be assigned to U.S. departments and agencies, contributing to an increasingly fragmented and congested spectrum, vulnerable to signal fratricide and intentional malicious interference. While modest bandwidths have been sufficient in the past, higher data rates, multiple beams, and higher transmit/receive gains are likely to be the norm for future commercial and government applications. Consequently, there is a critical need for ultra-wideband (UWB) communication systems.

To keep up with the aforementioned evolving needs there is strong interest to develop newer and more efficient hardware infrastructure and protocols. One enabling infrastructure is that of Radio Frequency (RF) front ends that are frequency agile, wideband, adaptable, very small in size and weight, and of small area and low power (SWAP). In addition, they include simultaneous time/frequency domain duplexing or simultaneous transmit and receive (STAR) or in-band full duplexing (IBFD). These technologies will allow for two-fold improvement in spectral efficiency [1], [2], [4], [5].

A typical STAR transceiver architecture is depicted in Fig. 1. Indeed, STAR radios can achieve in-band full

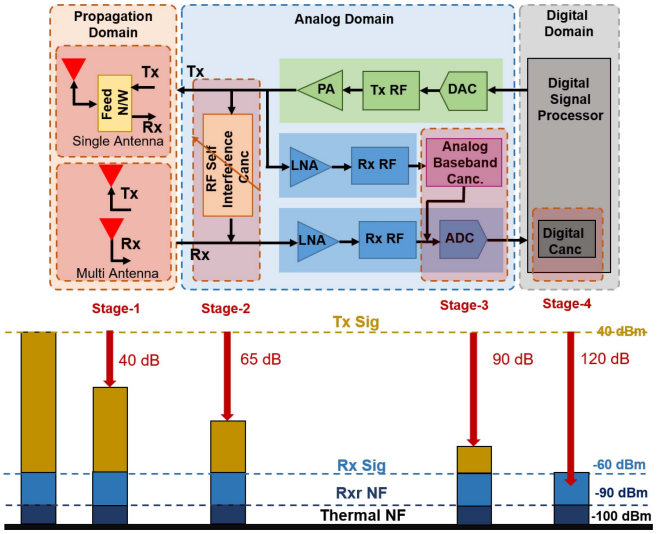

FIGURE 1. (Top) Detailed block diagram showing typical STAR radio implementation with 4-stages of cancellation across 3 domains. (Bottom) Tx and Rx signal power levels with achieved cancellation along the Rx chain.

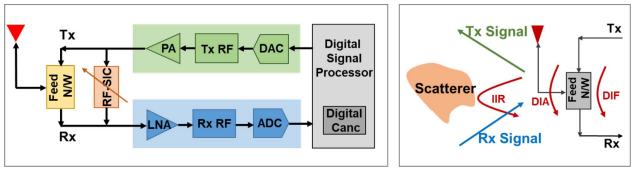

FIGURE 2. (Left) Single Antenna STAR radio realization with two stages of cancellation. (Right) Possible Tx interference signal components in single antenna radios.

duplexing to increase spectral efficiency. However, a major challenge in STAR realization is the coupling of high power transmit (Tx) signal onto the adjacent/co-located receive (Rx) channel(s). These coupled signals, if not suppressed, lead to desensitization and saturation of the receiver, specifically the low noise amplifier (LNA) and analog to digital converters (ADC). To suppress the coupled high power Tx signal, at least $100-120$ dB cancellation is required across the entire operational bandwidth [5]–[8]. In addition, the coupled signal may include multiple Tx signal components, namely 1) direct interference (original Tx signal) from the transmitter, 2) harmonics from power amplifiers (PA) in the Tx chain, 3) multi-path transmitted signals, and 4) noise from the transmit chain.

To achieve the desired suppression, multiple cancellation stages are required. Fig. 1, shows four cancellation stages. 1) Signal cancellation at the antenna stage, 2) analog radio frequency (RF) filters for RF cancellation, 3) analog baseband (BB) cancellation, and 4) digital cancellation [5], [6], [9]–[11]. Notably, the first 2 stages should provide at least 60 dB cancellation to prevent the receiver chain from being saturated.

Recent STAR realizations [6], [12]–[15], [15]–[22] have successfully demonstrated 80 - 110 dB interference suppression. However, this was achieved over a narrow bandwidth ($<$ 80 MHz) using not more than three cancellation stages. To overcome this shortcoming, a novel wideband STAR radio with 4 stages of cancellation was proposed in [7], [9], [23]. This STAR radio can achieve an unprecedented $\sim$ 120 dB of self-interference cancellation (SIC) across a bandwidth of 500 MHz. Of importance is the radios capability to cancel all linear, non-linear and transmit noise over the entire wide operational bandwidth.

Building on previous STAR radio realizations, in this paper, we review different and improved STAR self-interference cancellation approaches in the RF domain. Specifically, we review cancellation techniques at the antenna stage (Stage-1) and at the RF front end (RF-FE) (Stage-2). This is done for two radio implementations: a) single antenna radio, and b)multi antenna radios. For both cases, the achieved cancellation levels is $\sim$ 60 dB across a wide bandwidth. Therefore, with the inclusion of additional cancellation stages, the proposed STAR methods are poised to achieve a total $>$100 dB isolation in a small form factor and across GHz bandwidth with tunabilty.

This paper is structured as follows. Section II describes the existing radio architectures and the challenges associated with STAR realization. Following this, Section III presents Stage-1 (antenna stage) cancellation techniques in a single antenna or multi antenna radio. Section III describes the novel feed network used to achieve improved isolation of $>$ 60dB. Subsequently, Section IV, presents Stage-2 (RF canceller) cancellation details, followed by measurements showing combining cancellation across two-stages.

II. STAR RADIO ARCHITECTURES

A. SINGLE ANTENNA RADIOS

Most common radios employ single antenna to minimize resources. With a single antenna radio, full duplex is achieved either by employing time division duplexing (TDD) or frequency division duplexing (FDD). These radios employ a single antenna for transmission and reception using a single feed network that divides the transmitter and receiver circuits as depicted in Fig. 2 (left) [24]–[27]. However, employing TDD or FDD implies double the time and/or frequency resource allocation. Notably, TDD radios employ circulators or isolators to achieve finite interference suppression between the Tx and Rx chains [28], [29]. On the other hand, FDD radios employ diplexers for frequency filtering. Consequently, a larger number of tunable diplexers is required for multi-band radios employing FDD. A major drawback is also the significant interference from common modules (circulator/isolator/diplexer) connecting the Tx and Rx chains.

Fig. 2 (right) shows 3 possible paths for the high power Tx signals to couple into the Rx chain. These paths can be further divided into direct or in-direct interference components. Direct interference refers to signals that are coupled back to the receiver through cables/interconnects within the radio. The 2 direct interference components are: 1) coupling from the feed network component (circulator/isolator/diplexer) due

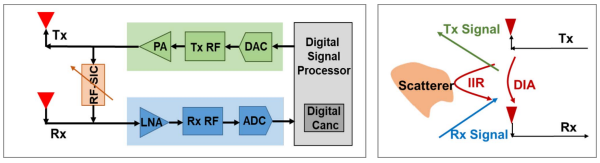

FIGURE 3. (Left) Multi Antenna STAR radio realization with two stages of cancellation. (Right) Possible Tx interference signal components in multi antenna radios.

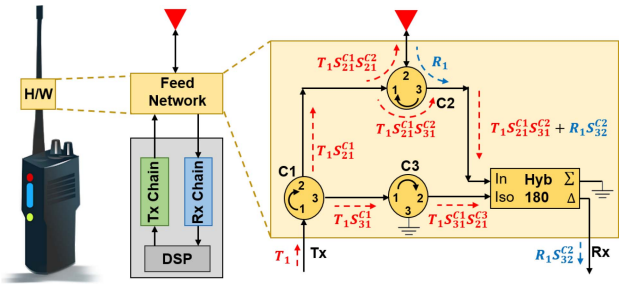

FIGURE 4. Single antenna feed network exploiting balanced feeding and symmetries to achieve improved cancellation.

to their finite isolation, referred to as *direct interference from feed* (DIF), and 2) reflection of Tx signals due to antenna mismatches, referred to as *direct interference from antenna* or DIA [30]. Direct interference signal components can be determined analytically and removed. But the removal of *in-direct interference from nearby reflectors*, referred to as IIR, is more challenging. Unlike direct interference signals, IIR signals are unpredictable and cannot therefore be accurately estimated apriori. In this paper, we present techniques to suppress direct interference components using the first 2 cancellation stages for single antenna and multi-antenna radios.

B. MULTI ANTENNA RADIOS

Multi antenna radios employing two or more antenna(s) are often used for specific applications. These antennas have separate chains for transmission and reception. As a result, they do not share a single feed network like the case with single antenna (see Fig. 3 (left)). However, multi antenna radios still suffer from direct and in-direct interference, as shown in Fig. 3 (right). DIA and IIR are the significant direct and in-direct interference components in this case.

To achieve improved isolation, different antenna isolation techniques must be applied in Stage-1, depending on the application. However, due to the proximity of multiple Tx antennas, these approaches do not provide the required 60 dB RF cancellation. Consequently, these radios are highly dependent on the RF cancellation stage to augment the limited antenna isolation. Together, the antenna and RF cancellation stages can achieve $>$ 60 dB of cancellation.

RF cancellation circuits are implemented using time domain approaches (with time delay and weights) or frequency domain approaches (with phase shifters and weights) [30], [31]. Implementation complexity of these RF cancellation circuits (in terms of filter order and components) is directly proportional to the desired cancellation at this stage. In other words, a higher order filter is required to provide more cancellation. Increase in filter order would result in influencing the inter-modulation products (IP3) and noise figure among other parameters, there by affecting the Rx chain performance [12], [31], [32]. Thus, it is desirable to achieve maximum cancellation (at least 35 dB) at the antennas there by relaxing the cancellation requirement at the RF filters.

III. STAGE-1 CANCELLATION

A. SINGLE ANTENNA RADIOS

As mentioned in Section II, for a single antenna radio, the isolation is limited to $\sim$ 20 dB depending on the circulator or diplexer isolation. However, it is expected to have a suppression on the order of 60 dB using the first two stages. To improve the achieved stage-1 isolation, we propose an antenna agnostic feed network technique that can provide 45–60 dB isolation. Below we present this new approach: Fig. 4 depicts the antenna agnostic feed network employing 3 identical circulators and a hybrid-180° coupler. It is assumed that the [S] parameters of all three circulators are identical.

The cancellation process is described as follows. The high power Tx signal (T_1) at the input of the feed network is fed to circulator C1, resulting in an output signal at ports 2 and 3, $T_1 S_{21}^{C1}$ and $T_1 S_{31}^{C1}$, respectively. The Port 2 output from C1 is fed to circulator C2 and then to the antenna. But the output from port 3 of C1 is fed to C3 and will be later used for cancelling the signal coupled into the receiver. As depicted, Circulator C2 feeds the antenna through port 2 with the Tx signal corresponding to $T_1 S_{21}^{C1} S_{21}^{C2}$. Finite isolation (typically 20 dB) between the ports at C2, results in a leakage signal from port 1 flowing into port 3, represented as $T_1 S_{21}^{C1} S_{31}^{C2}$. This high power signal, otherwise present in a conventional transceiver, is the signal of interest to be suppressed. Maintaining perfect symmetry between two input paths of hybrid-180° coupler, results in achieving maximum cancellation. That is, the output of the hybrid-180° coupler contain only the desired Rx signal $R_1 S_{32}^{C2}$ and no residual transmit signal. It should be noted that a balun could also be used in place of a hybrid-180° coupler.

Assuming all the components are matched perfectly with negligible insertion loss ($S_{21}^{C1} = 1$), the signal component corresponding to $T_1 S_{31}^{C1}$ needs to be suppressed. Signal components at the outputs of C2 and C3 are represented as $T_1 S_{21}^{C1} S_{31}^{C2}$ and $T_1 S_{31}^{C1} S_{21}^{C3}$, respectively. However, non-idealities in devices and in the signal paths lead to amplitude and/or phase imbalances between both paths. Slightest amplitude and phase variation will lead to degradation in cancellation levels. Considering the Tx signal component alone, analytically, the output from hybrid-180° coupler can be expressed as,

$$R_1 = T_1 S_{21}^{C1} S_{31}^{C2} \alpha e^{j\theta} - T_1 S_{31}^{C1} S_{21}^{C3} \quad (1)$$

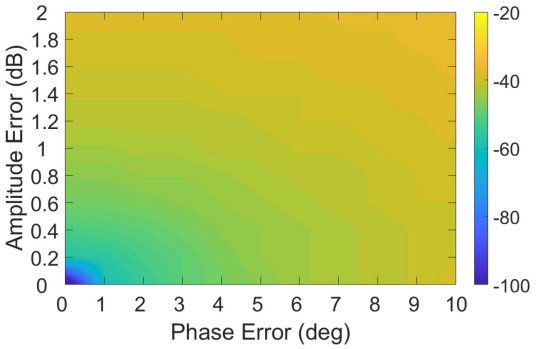

FIGURE 5. Effect of amplitude and phase imbalance on achieved cancellation.

where, α corresponds to cumulative amplitude imbalance and θ corresponds to cumulative phase imbalance, between the two input signal to hybrid-180° coupler. Under the assumption that $S_{21}^{C1} = S_{21}^{C3}$ and $S_{31}^{C1} = S_{31}^{C2}$, the above equation can be reduced to,

$$R_1 = T_1 S_{21} S_{31} \left(\alpha e^{j\theta} - 1 \right) \tag{2}$$

The effect of amplitude and phase imbalance can be seen in Fig. 5. In the above equation, when there is no amplitude imbalance (0 dB or $\alpha = 1$) and no phase imbalance ($\theta = 0$), the above equation reduces to $R_1 = 0$. On the other hand, for example, an amplitude variation of 1 dB and phase imbalance of 4^0 results in achieved cancellation dropping to -40 dB. It should be noted that the term corresponding to $(\alpha e^{j\theta} - 1)$ represents the achieved cancellation of the isolated signal ($T_1 S_{31}$), which otherwise would be present in a typical receiver.

To validate the above approach, a simple feed network was realized using existing commercial-off-the-shelf (COTS) components as shown in Fig. 7(a). In addition, a balun was employed in place of hybrid-180° coupler during measurements. Measured performance of COTS circulator (PE83CR004) and balun (BAL-0003) are presented in Fig. 6. The transmit signal T_1 encounters, insertion loss (S_{21}^{C1}) and isolation (S_{31}^{C1}) from circulator C1. As the signal progresses through circulator C2, it undergoes further isolation (S_{31}^{C2}). Similarly, the other part of the signal from C1 undergoes insertion loss (S_{21}^{C3}) from circulator C3. Consequently, only the magnitude and phase responses for these 4 components are plotted in Fig. 6. The insertion loss of both input ports of balun coupler are also plotted. In addition, the amplitude and phase mismatches between corresponding ports are also plotted. It should be noted that solid lines and dotted lines represent two different device measurements. As seen in Fig.6, measured insertion loss of circulators is 0.5 dB and that of balun is 7 dB. It should be noted that the employed COTS components had a return loss of < -20 dB across the band of interest ($1.8 - 2.2$ GHz). This specific operational band between $1.8 - 2.2$ GHz was chosen for demonstration due to stable insertion loss and improved isolation.

Fig. 7(b) demonstrates that the total transmit signal power is suppressed by at least 60 dB across the desired bandwidth

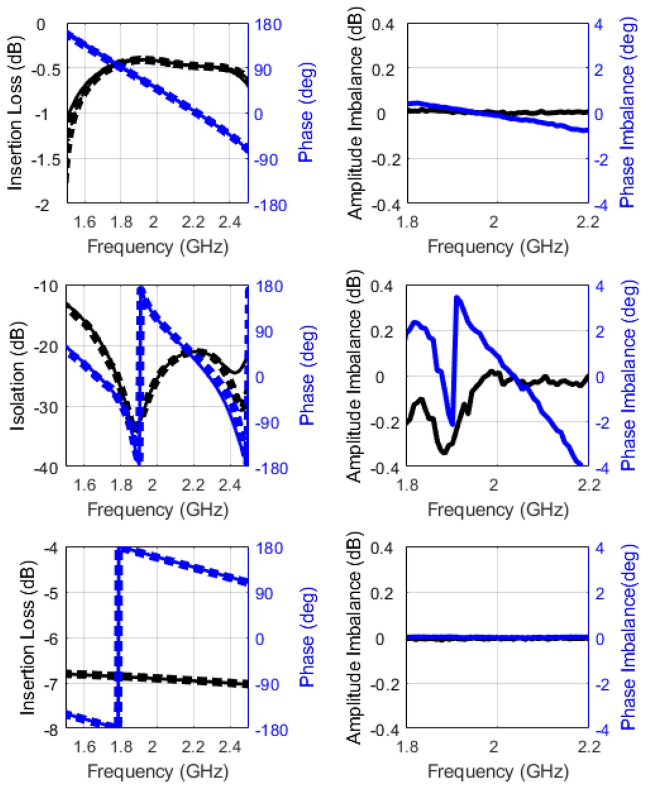

FIGURE 6. (Top Left) Measured insertion loss S_{21}^{C1} S_{21}^{C3}, (middle left) measured isolation S_{31}^{C1} S_{31}^{C2}, (bottom left) measured insertion loss S_{21} S_{31} input ports of balun, and their corresponding amplitude and phase mismatches (right). All amplitude plots are depicted in black and phase plots are depicted in blue.

(BW) of 400 MHz. This cancellation is limited by the COTS operation. Importantly, this approach results in 40 dB additional suppression of residual transmit signal power over existing circulators with additional benefits, namely: 1) ease of integration into existing radios, irrespective of antenna type, 2) suppression of all signal components from the transmit chain (high power direct transmit signals, harmonics from power amplifiers, and noise coupling from the transmit chain), and 3) enables SWaP-C implementation due to its passive nature with no power consumption.

It should be noted that the measurements were performed to prove that feed network with circulators can provide the desired cancellation for a well-matched antenna over narrowband(s). However, for the measurement, due to the unavailability of a single wideband antenna (400 MHz) with $S_{11} < -30$ dB across the entire band, we used a 50Ω load to emulate multiple narrowband antennas across 400 MHz. Further, the antenna impedance matching influences the achieved cancellation to a great extent. Consequently, the antenna connected to port-2 of circulator-2 should be well matched to achieve increased isolation, as shown in Fig. 8.

B. MULTI ANTENNA RADIOS

In this section, we discuss five different techniques to improve antenna isolation. These include techniques such as exploitation of polarization diversity, physical separation

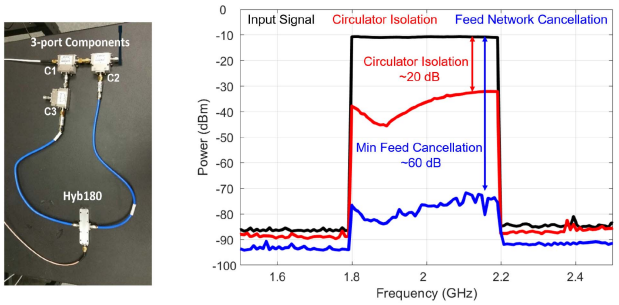

FIGURE 7. (a) COTS implementation of proposed high isolation feed network, and (b) Measured cancellation levels using the proposed feed network (blue) and standard circulator (Red).

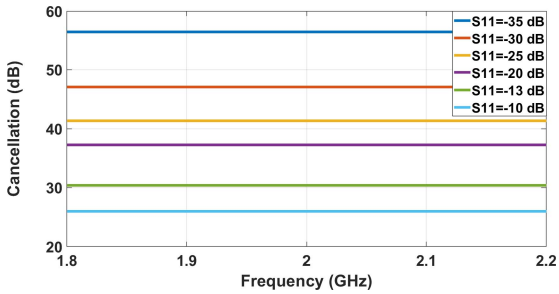

FIGURE 8. Simulation showing degradation in achieved cancellation as a function of antenna impedance mismatch under ideal conditions.

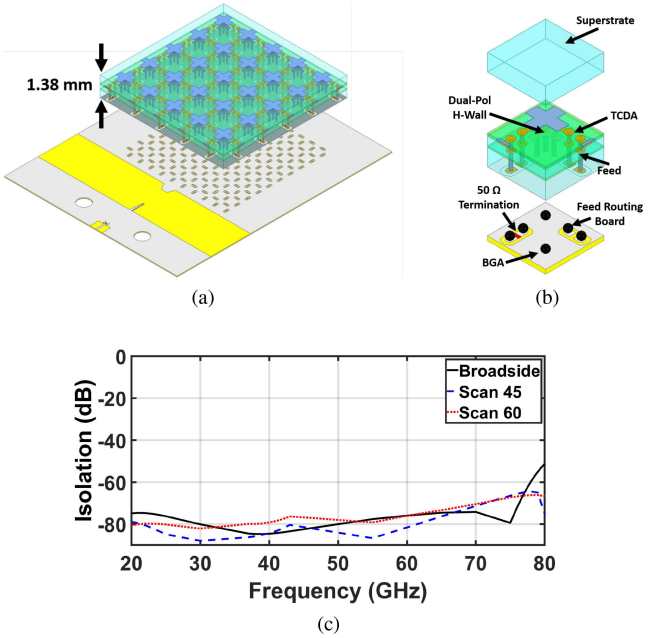

FIGURE 9. (a) Modeled dual polarized mmWave TCDA containing twin line feed and H-wall used to push scan-dependent common-modes out of band, (b) Unit cell stack up, and (c) simulated port isolation at different scan angles.

between co-located antennas, FSS/EBG structures for decoupling antennas, antenna enclosure within cavities or parasitic walls and inclusion of tunable elements to achieve structural symmetry in phase and magnitude.

Techniques have also been studied for increasing isolation between antenna array elements. Examples include employing a linear array for digital beamforming [33] to reduce Tx/Rx coupling in across 125 MHz, a 2×2 patch antenna array [34] using narrowband filters provides 30 dB isolation across a 110 MHz bandwidth. However, previous implementations of inter element coupling are narrowbands with limited scanning efficiency. Isolation Improvements have been considered, but these were limited to broadside arrays [35]. With this in mind, this section focuses on high isolation wide bandwidth STAR antenna arrays with wide angle scanning. It should be noted that the focus of this paper is to briefly summarize characterized high isolation antenna implementations.

1) POLARIZATION DIVERSITY

By employing polarization diversity adjacent or collocated antenna elements have reduced coupling. Achieving this reduced coupling or isolation across a large bandwidth is even more challenging.

a) *Linear polarization:* Achieving improved isolation using orthogonal polarization greatly depends on the symmetry of the antennas, and their feeds. To achieve this even when scanning, a first step is to choose an UWB radiator, such as a dual-linear polarized tightly coupled dipole array (TCDA). TCDAs have demonstrated large impedance bandwidths and high cross-polarized isolation of 40 dB in simulation even under scanning [36]–[38].

To improve operational bandwidth, Marchand Balun feeds have been used, but these feed are inherently not symmetric. As a result, measurements show only 20 dB isolation between Tx/Rx [36]. Alternately, use of differential feed allows for better symmetry, thus, improving isolation between the dual polarized antenna elements. Further, differential feeds have lower noise in the transceiver chain.

To improve feed symmetry, a UWB differentially twin line fed for mm-wave aperture was presented in [39] (see Fig. 9). This feed is achieved using balanced transmission lines causing current in opposite phases. Indeed, this symmetry leads to low cross-polarized isolation of $\sim$ 60 dB as shown in Fig. 9(c). Full wave simulations show that a VSWR < 3 was achieved across 22-80 GHz, with scanning down to 45°. It should be noted that this array scales to lower frequency with similar levels of isolation using a differential feeding approach.

b) *Circular polarization:* Circular polarization is preferred in certain cases as it leads to lower polarization mismatches. Indeed, slot spiral antennas [40] are known for their excellent circularly polarized (CP) radiation, low profile and wideband performance.

However, to design a wideband beam steering spiral array, there are several key challenges to overcome. First, the spiral element must be miniaturized to achieve no grating lobe across larger bandwidths [41]. Often, the spiral diameter is larger to minimise reflections from the spiral arm terminations. To avoid this issue, a single matched resistor is

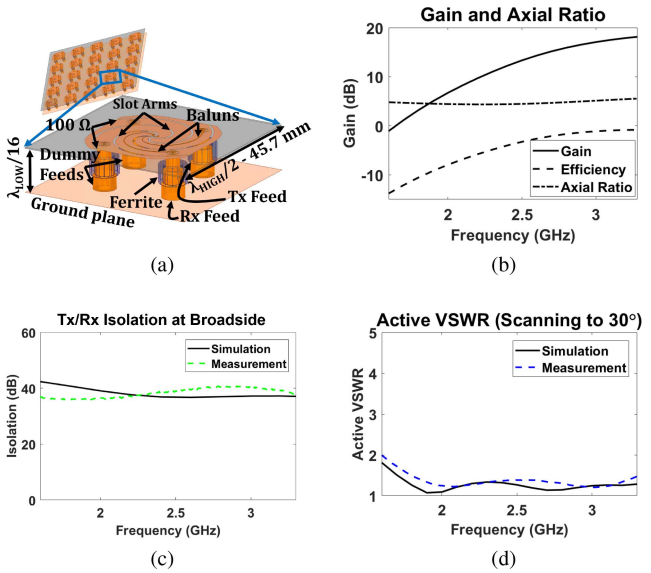

FIGURE 10. (a) Wideband 25-element 4-arm spiral array with high isolation (unit-cell depicted) with feeding and Balun transformation implementation, (b) Gain, efficiency and axial ratio of the spiral antenna, (c) measured Tx/Rx isolation averaged 35 dB across 2-5 GHz, and (d)active VSWR was < 2.5 even when scanning.

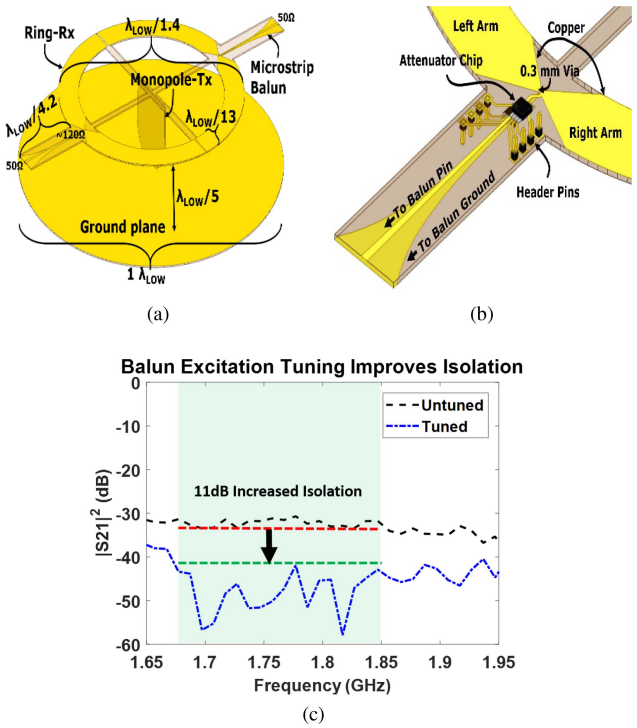

FIGURE 11. (a) High Tx/Rx isolation antenna exhibits wideband operation, (b) The balun with analog amplitude control enables greater inherent antenna isolation, and (c) Isolation improved by > 11dB across a 200 MHz bandwidth.

introduced at the end of each slot arm to suppress reflections. Also, a balanced feeding was introduced to suppress interference between the Tx and Rx arms of the subject 4-arm spiral. The 50Ω to 120Ω in microstrip infinite balun was used in [40] to achieve balanced feeding. Notably, no separate balun was required, with significantly SWAP-C reduction as shown in Fig. 10(b). To ensure structural symmetry, dummy coaxial feed was added as well. This led to higher isolation than previously recorded arrays of the same type.

Full wave simulations of 4-arm spiral arrays showed a high isolation of >40 dB, achieved from 1-5 GHz (5 : 1 bandwidth). This isolation was ∼11 dB less at 30° scanning. A 3×3 finite array simulation produced similar results (see Fig. 10(a)). Also, measurements confirmed these simulations showing a 35 dB average Tx/Rx isolation. When scanning down to 30°, this isolation was reduced by a maximum of ∼9 dB (see Fig. 10(b)). In terms of VSWR, no appreciable degradation was found across the entire bandwidth while scanning. Notably, a dual-pol linear antenna has orthogonal polarizations, however, in case of a four-arm spiral both antennas transmit the same polarization, either RHCP or LHCP [35].

2) EXPLOITING AMPLITUDE AND PHASE BALANCE

Another way to improve isolation in a multi-antenna radio is to employ a tunable balun that compensates for amplitude imbalances between the antenna feed branches. Above, we discussed use of symmetric structure and balanced feeding. However, the isolation level using this approach can be limited due to structural imperfections and manufacturing tolerances. This issue can be addressed using tunable baluns.

The concept of using tunable baluns is depicted Fig. 11(a). In this case, a microstrip feed with a tapered ground plane is used to feed a circular loop. The feed is an exponential tapered microstrip balun which is 45 mm long. To determine the approximate amplitude imbalance of the balun two back-to-back baluns were fabricated. One balun had inverted polarities connected (i.e., signal-ground of one balun connected to ground-signal of the other, respectively). The difference in S_{21} for the two baluns is the estimated via measurements.

To compensate for the current imbalance in the balun, an attenuator chip was inserted in each arm of the balun. The attenuator in the chip is controlled by a DC voltage bias. Specifically, while the antenna is in operation, the resistor value is altered via the bias voltage to achieve amplitude and phase current control within the balun's arm. It should be noted that the insertion loss of the employed balun is 1.2 dB. Measurements indicate that reliable control the attenuation by steps of <0.1 dB, is possible. Fig. 11(c) shows that this resistor chip insert leads to 11 dB improvement in isolation. This resulted in an overall antenna isolation of >45 dB across a wideband operation. A major advantage using the attenuator chip is its selective tuning across a selected range of frequencies.

3) OTHER DECOUPLING TECHNIQUES

Physical separation is the simplest way to decouple a Tx and Rx antenna to reduce inter-element coupling. However, this approach adds to size and is not suited for arrays [17].

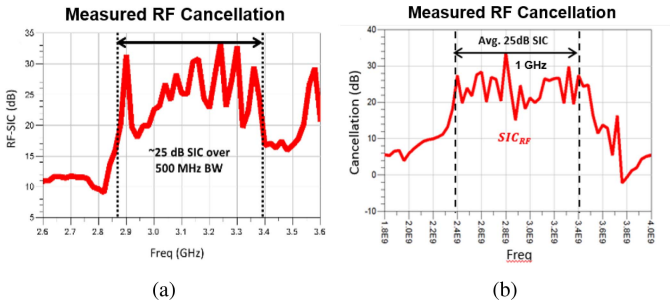

FIGURE 12. (a) Achieved cancellation of > 20 dB across 500 MHz using 6-tap RF-FIR filter, (b) Achieved cancellation of > 20 dB across 1 GHz using 12-tap RF-FIR filter bank.

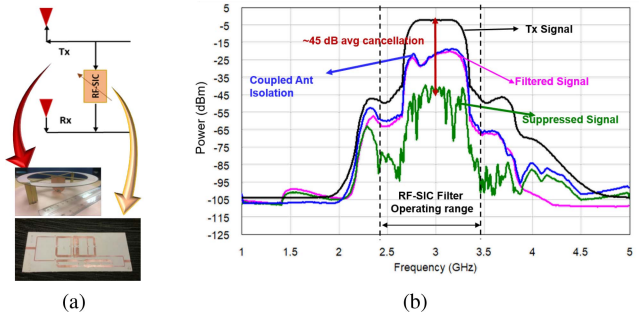

FIGURE 13. (a) Employed dual antenna and 1 GHz RF-SIC filter for combined cancellation, (b) Achieved two-stage combined cancellation showing an average cancellation of 50 dB over 1 GHz BW.

To avoid size and cost issues insert can be used to make the antenna to antenna separation electrically (not physically) larger. The simplest form of this approach is to use high permittivity and/or high permeability substrates. Another effective method is the introduction of periodic structures, either Frequency Selective surfaces (FSS), or Electro-Band-Gap (EBG) structures, or high impedance surfaces that reject certain frequencies from propagating between antennas [42]–[44].

Using periodic structures, a wideband, bi-static, and dual-polarized simultaneous transmit and receive antenna subsystem was demonstrated with isolation >60 dB across 6-19 GHz band. Specifically, a high capacitive reactance bed of "nails" was used to suppress TM polarized surface waves [45].

Another method of attenuating coupling signal between antennas is to use a brute force attenuation or shielding of the adjacent elements. Techniques such as cavities, resistive walls, and lossy magnetics, can reduce coupling between adjacent elements at the cost of efficiency and space [46], [47].

IV. STAGE-2: RF CANCELLATION

Additional cancellation of direct interference signals into the receiver can be achieved at the RF stage (See Fig. 1). This stage employs static or tunable filters to suppress interference from the Tx or exterior regions. In this paper, we consider time domain RF canceller implementations that can be used for single and multi antenna STAR radios.

A. STATIC RF CANCELLER

As noted in Section II, we need at least two stages of RF to achieve 60 dB cancellation or more. Consequently, stage-2 should provide an additional 20 to 25 dB SIC across the operational bandwidth. RF canceller is realized using a multi-tap finite impulse response (FIR) filter. Each tap consists of a pair of tunable amplitude and phase components with delay lines. Previous such filters were inherently narrowband [4], [6], [31] and less tunable as they included only limited delay lines. In [7], [9], [23], we implemented static RF-FIR prototypes to achieve at least 20 dB cancellation across 500 MHz and 1 GHz. But by increasing the number of taps in a filter more variables are available for optimization, thus improving the cancellation bandwidth.

The goal of any RF-FIR filter is to cancel the power coupled from the Tx signal to RF section of the receiver chain. This coupled signal can be represented by the transfer function $H_{chnl}(j\omega)$. Notably, the antenna response $H_{chnl}(j\omega)$ accounts for all direct interference signal components. Therefore, the goal is to cancel this coupled interference signal. To do so, the aim is to develop a RF canceller with a transfer function,

$$H_{fil}(j\omega) = \sum_{k=0}^{K-1} b_k e^{-j\omega\tau_k} \tag{3}$$

In this, b_k and τ_k are the taps and delay values. By choosing appropriately the coefficients b_k and τ_k, $H_{chnl}(j\omega) = -H_{fil}(j\omega)$ can be achieved across the entire bandwidth and therefore cancel the coupled signal into the RF domain.

The level of self-interference cancellation can be computed from,

$$SIC_{RF}|_{(dB)} = 20log_{10}\frac{H_{fil}(j\omega) + H_{chnl}(j\omega)}{\sqrt{2}H_{chnl}(j\omega)} \tag{4}$$

Fig. 12 demonstrates the RF-FIR filter cancellation level using a fabricated prototype. As can be seen, the fabricated RF-FIR filter provides at least 20 dB cancellation across the entire bandwidth and by increasing the number of taps, it is possible to further increase the cancellation bandwidth and/or cancellation magnitude.

V. TWO STAGE COMBINED CANCELLATION

Overall, the combined cancellation achieved using two stages of cancellation in single antenna and multi-antenna radios was shown to be 50 dB, as shown in Fig. 13. To evaluate the cancellation over wideband, the measurement was performed using a multi-antenna setup in an anechoic chamber with little to no variation in the surrounding environment. For this, a high isolation dual-antenna was considered, operating between $1.9 - 4$ GHz. A 12-tap RF-SIC filter providing at least 20 dB cancellation across 1 GHz bandwidth (see Fig. 12(b)) was employed in conjunction with this antenna. The combined cancellation is shown in Fig. 13(b). The plot

shows the power spectrum of 4 signals; a) Tx input signal, b) suppressed signal due to antenna, c) RF-FIR filtered signal, and d) two-stage cancelled signal. Additional stages can be included to further improve cancellation, as shown in Fig. 1. However, these cancellation techniques are beyond the scope of this paper.

VI. CONCLUSION

In this paper, we summarized approaches employed by our team to achieve improved cancellation across a wideband using stage-1 and stage-2 for a single antenna and multi-antenna STAR radios. Specifically, we presented antenna isolation techniques for large arrays and presented a novel feed network that can be employed for single antenna STAR radios. Both stage-1 approaches provided cancellation of $\sim$ 35 dB at the antenna level. Following this, in stage-2, we presented static and tunable RF canceller. Measured results using 2 static RF canceller prototype showed achievable direct interference cancellation of at least 20 dB over 500 MHz and 1 GHz. Using the above mentioned approaches, the combined first 2 stage cancellation of $>$ 60 dB over the entire 500 MHz, was achieved.

ACKNOWLEDGMENT

The authors would like to thank Dr. Markus Novak and MaXentric Technologies.

REFERENCES

[1] S. Hong *et al.*, "Applications of self-interference cancellation in 5G and beyond," *IEEE Commun. Mag.*, vol. 52, no. 2, pp. 114–121, Feb. 2014.

[2] A. Sabharwal, P. Schniter, D. Guo, D. W. Bliss, S. Rangarajan, and R. Wichman, "In-band full-duplex wireless: Challenges and opportunities," *IEEE J. Sel. Areas Commun.*, vol. 32, no. 9, pp. 1637–1652, Sep. 2014.

[3] L. Larson, "RF and microwave hardware challenges for future radio spectrum access," *Proc. IEEE*, vol. 102, no. 3, pp. 321–333, Mar. 2014.

[4] K. E. Kolodziej, J. G. McMichael, and B. T. Perry, "Multitap RF canceller for in-band full-duplex wireless communications," *IEEE Trans. Wireless Commun.*, vol. 15, no. 6, pp. 4321–4334, Jun. 2016.

[5] D. Bharadia and S. Katti, "Full duplex MIMO radios," in *Proc. 11th USENIX Conf. Netw. Syst. Design Implement.*, 2014, pp. 359–372.

[6] D. Bharadia, E. McMilin, and S. Katti, "Full duplex radios," in *Proc. Conf. SIGCOMM ACM*, New York, NY, USA, 2013, pp. 375–386.

[7] S. Bojja Venkatakrishnan, E. A. Alwan, and J. L. Volakis, "Wideband RF self-interference cancellation circuit for phased array simultaneous transmit and receive systems," *IEEE Access*, vol. 6, pp. 3425–3432, 2018.

[8] T. Dinc and H. Krishnaswamy, "A T/R antenna pair with polarization-based reconfigurable wideband self-interference cancellation for simultaneous transmit and receive," in *Proc. IEEE MTT-S Int. Microw. Symp.*, May 2015, pp. 1–4.

[9] S. Bojja-Venkatakrishnan, E. A. Alwan, and J. L. Volakis, "Simultaneous transmit and receive system with 1 GHz RF cancellation bandwidth," in *Proc. IEEE Int. Symp. Antennas Propag. USNC/URSI Nat. Radio Sci. Meeting*, 2018, pp. 1241–1242.

[10] K. L. Scherer *et al.*, "Simultaneous transmit and receive system architecture with four stages of cancellation," in *Proc. IEEE Int. Symp. Antennas Propag. USNC/URSI Nat. Radio Sci. Meeting*, Jul. 2015, pp. 520–521.

[11] A. Hovsepian, S. B. Venkatakrishnan, E. A. Alwan, and J. L. Volakis, "Wideband beam steering using a 4-arm spiral array for simultaneous transmit and receive (STAR) operation," in *Proc. IEEE Int. Symp. Antennas Propag. USNC/URSI Nat. Radio Sci. Meeting*, Jul. 2018, pp. 1915–1916.

[12] J. Zhou and H. Krishnaswamy, "System-level analysis of phase noise in full-duplex wireless transceivers," *IEEE Trans. Circuits Syst. II, Exp. Briefs*, vol. 65, no. 9, pp. 1189–1193, Sep. 2018.

[13] M. Duarte and A. Sabharwal, "Full-duplex wireless communications using off-the-shelf radios: Feasibility and first results," in *Proc. Conf. Rec. 44th Asilomar Conf. Signals Syst. Comput.*, Nov. 2010, pp. 1558–1562.

[14] D. J. van den Broek, E. A. M. Klumperink, and B. Nauta, "A self-interference-cancelling receiver for in-band full-duplex wireless with low distortion under cancellation of strong TX leakage," in *Proc. IEEE Int. Solid-State Circuits Conf. (ISSCC) Dig. Techn. Papers*, Feb. 2015, pp. 1–3.

[15] S. Chen, M. A. Beach, and J. P. McGeehan, "Division-free duplex for wireless applications," *Electron. Lett*, vol. 34, no. 2, pp. 147–148, Jan 1998.

[16] M. Jain *et al.*, "Practical, real-time, full duplex wireless," in *Proc. 17th Annu. Int. Conf. Mobile Comput. Netw.*, 2011, pp. 301–312.

[17] E. Everett, A. Sahai, and A. Sabharwal, "Passive self-interference suppression for full-duplex infrastructure nodes," *IEEE Trans. Wireless Commun.*, vol. 13, no. 2, pp. 680–694, Feb. 2014.

[18] B. Debaillie *et al.*, "Analog/RF solutions enabling compact full-duplex radios," *IEEE J. Sel. Areas Commun.*, vol. 32, no. 9, pp. 1662–1673, Sep. 2014.

[19] N. Reiskarimian *et al.*, "One-way ramp to a two-way highway: Integrated magnetic-free nonreciprocal antenna interfaces for full-duplex wireless," *IEEE Microw. Mag.*, vol. 20, no. 2, pp. 56–75, Feb. 2019.

[20] M. Biedka, Y. E. Wang, Q. M. Xu, and Y. Li, "Full-duplex RF front ends: From antennas and circulators to leakage cancelation," *IEEE Microw. Mag.*, vol. 20, no. 2, pp. 44–55, Apr. 2020.

[21] I. Brodsky, J. Brand, and M. Jain, "Freedom of frequency: How the quest for in-band full-duplex led to a breakthrough in filter design," *IEEE Microw. Mag.*, vol. 20, no. 2, pp. 36–43, Feb. 2019.

[22] M. Katanbaf, K. Chu, T. Zhang, C. Su, and J. C. Rudell, "Two-way traffic ahead: RF/analog self-interference cancelation techniques and the challenges for future integrated full-duplex transceivers," *IEEE Microw. Mag.*, vol. 20, no. 2, pp. 22–35, Feb. 2019.

[23] S. Bojja-Venkatakrishnan, E. A. Alwan, and J. L. Volakis, "Wideband RF and analog self-interference cancelation filter for simultaneous transmit and receive system," in *Proc. IEEE Int. Symp. Antennas Propag. USNC/URSI Nat. Radio Sci. Meeting*, Jul. 2017, pp. 933–934.

[24] M. B. Dastjerdi, S. Jain, N. Reiskarimian, A. Natarajan, and H. Krishnaswamy, "Analysis and design of a full-duplex two-element MIMO circulator-receiver with high TX power handling exploiting MIMO RF and shared-delay baseband self-interference cancellation," *IEEE J. Solid-State Circuits*, vol. 54, no. 12, pp. 3525–3540, Dec. 2019.

[25] A. Nagulu and H. Krishnaswamy, "Non-magnetic CMOS switched-transmission-line circulators with high power handling and antenna balancing: Theory and implementation," *IEEE J. Solid-State Circuits*, vol. 54, no. 5, pp. 1288–1303, May 2019.

[26] A. Kord, M. Tymchenko, D. L. Sounas, H. Krishnaswamy, and A. Alù, "CMOS integrated magnetless circulators based on spatiotemporal modulation angular-momentum biasing," *IEEE Trans. Microw. Theory Techn.*, vol. 67, no. 7, pp. 2649–2662, Feb. 2019.

[27] N. Reiskarimian, M. B. Dastjerdi, J. Zhou, and H. Krishnaswamy, "Analysis and design of commutation-based circulator-receivers for integrated full-duplex wireless," *IEEE J. Solid-State Circuits*, vol. 53, no. 8, pp. 2190–2201, Aug. 2018.

[28] H. Holma, S. Heikkinen, O. A. Lehtinen, and A. Toskala, "Interference considerations for the time division duplex mode of the UMTS terrestrial radio access," *IEEE J. Sel. Areas Commun.*, vol. 18, no. 8, pp. 1386–1393, Aug. 2000.

[29] H. Haas and G. J. R. Povey, "The effect of adjacent channel interference on capacity in a hybrid TDMA/CDMA-TDD system using UTRA-TDD parameters," in *Proc. IEEE VTS 50th Veh. Technol. Conf. (VTC-Fall)*, vol. 2, 1999, pp. 1086–1090.
[30] K. E. Kolodziej, B. T. Perry, and J. S. Herd, "In-band full-duplex technology: Techniques and systems survey," *IEEE Trans. Microw. Theory Techn.*, vol. 67, no. 7, pp. 3025–3041, Jul. 2019.
[31] J. Zhou, T. H. Chuang, T. Dinc, and H. Krishnaswamy, "Integrated wideband self-interference cancelation in the RF domain for FDD and full-duplex wireless," *IEEE J. Solid-State Circuits*, vol. 50, no. 12, pp. 3015–3031, Dec. 2015.
[32] Z. Zhang, K. Long, A. V. Vasilakos, and L. Hanzo, "Full-duplex wireless communications: Challenges, solutions, and future research directions," *Proc. IEEE*, vol. 104, no. 7, pp. 1369–1409, 2016.
[33] J. P. Doane, K. E. Kolodziej, and B. T. Perry, "Simultaneous transmit and receive with digital phased arrays," in *Proc. IEEE Int. Symp. Phased Array Syst. Technol. (PAST)*, Oct. 2016, pp. 1–6.
[34] A. T. Wegener, "Broadband near-field filters for simultaneous transmit and receive in a small two-dimensional array," in *Proc. IEEE MTT-S Int. Microw. Symp. (IMS)*, Jun. 2014, pp. 1–3.
[35] E. A. Etellisi, M. A. Elmansouri, and D. S. Filipovic, "Wideband monostatic simultaneous transmit and receive (STAR) antenna," *IEEE Trans. Antennas Propag.*, vol. 64, no. 1, pp. 6–15, Jan. 2016.
[36] J. Zhong, A. Johnson, E. A. Alwan, and J. L. Volakis, "Dual-linear polarized phased array with 9:1 Bandwidth and 60° scanning off broadside," *IEEE Trans. Antennas Propag.*, vol. 67, no. 3, pp. 1996–2001, Mar. 2019.
[37] E. Yetisir, C.-C. Chen, and J. L. Volakis, "Low-profile UWB 2-port antenna with high isolation," *IEEE Antennas Wireless Propag. Lett.*, vol. 13, pp. 55–58, 2014.
[38] E. Yetisir, N. Ghalichechian, and J. L. Volakis, "Ultrawideband array with 70^0 scanning using FSS superstrate," *IEEE Trans. Antennas Propag.*, vol. 64, no. 10, pp. 4256–4265, Oct. 2016.
[39] A. D. Johnson, S. B. Venkatakrishnan, E. A. Alwan, and J. L. Volakis, "Suppressing E-plane scan resonance for UWB millimeter-wave differential phased array," in *Proc. Int. Appl. Comput. Electromagn. Soc. Symp. (ACES)*, Apr. 2019, pp. 1–2.
[40] J. L. Volakis, M. W. Nurnberger, and D. S. Filipovic, "Slot spiral antenna," *IEEE Antennas Propag. Mag.*, vol. 43, no. 6, pp. 15–26, Dec. 2001.
[41] B. A. Kramer, M. Lee, C.-C. Chen, and J. L. Volakis, "Design and performance of an ultrawide-band ceramic-loaded slot spiral," *IEEE Trans. Antennas Propag.*, vol. 53, no. 7, pp. 2193–2199, Jul. 2005.
[42] M. Akbari, H. A. Ghalyon, M. Farahani, A. Sebak, and T. A. Denidni, "Spatially decoupling of CP antennas based on FSS for 30-GHz MIMO systems," *IEEE Access*, vol. 5, pp. 6527–6537, 2017.
[43] X. Yang, Y. Liu, Y. Xu, and S. Gong, "Isolation enhancement in patch antenna array with fractal UC-EBG structure and cross slot," *IEEE Antennas Wireless Propag. Lett.*, vol. 16, pp. 2175–2178, 2017.
[44] T. Dabas, D. Gangwar, B. K. Kanaujia, and A. Gautam, "Mutual coupling reduction between elements of UWB MIMO antenna using small size uniplanar EBG exhibiting multiple stop bands," *AEU Int. J. Electron. Commun.*, vol. 93, pp. 32–38, Sep. 2018. [Online]. Available: http://www.sciencedirect.com/science/article/pii/S1434841117328352
[45] P. V. Prasannakumar, M. A. Elmansouri, and D. S. Filipovic, "Wideband decoupling techniques for dual-polarized bi-static simultaneous transmit and receive antenna subsystem," *IEEE Trans. Antennas Propag.*, vol. 65, no. 10, pp. 4991–5001, Oct. 2017.
[46] G. Zhai, Z. N. Chen, and X. Qing, "Mutual coupling reduction of a closely spaced four-element MIMO antenna system using discrete mushrooms," *IEEE Trans. Microw. Theory Tech.*, vol. 64, no. 10, pp. 3060–3067, Oct. 2016.
[47] G. Zhai, Z. N. Chen, and X. Qing, "Enhanced isolation of a closely spaced four-element MIMO antenna system using metamaterial mushroom," *IEEE Trans. Antennas Propag.*, vol. 63, no. 8, pp. 3362–3370, Aug. 2015.

SATHEESH BOJJA VENKATAKRISHNAN (Member, IEEE) was born in Tiruchirappalli, India, in 1987. He received the bachelor's degree in electronics and communication engineering from the National Institute of Technology, Tiruchirappalli, in 2009, and the M.S. and Ph.D. degrees in electrical engineering from the Ohio State University, Columbus, OH, USA, in 2017.

He was a Scientist with DRDO, India, from 2009 to 2013, working on the development and implementation of active electronic steerable antennas. He is currently a Research Assistant Professor of electrical and computer engineering with Florida International University. His current research includes receiver design for communication circuits, RF systems, and digital signal processing using FPGAs. He is also working on simultaneous transmit and receive system (STAR), to improve the spectral efficiency. He was an IEEE Electromagnetic Theory Symposium Young Scientist Award recipient in 2019. He won the 2nd prize in International Union of Radio Science General Assembly and Scientific Symposium (URSI-GASS) Student Paper Competition, in August 2017. He also received Honorable Mention in the Student Paper Competition at the IEEE Antenna and Propagation Symposium (AP-S/URSI) in 2015 and 2016, and the Student Fellowship Travel Grant Award at the U.S. National Committee for the International Union of Radio Science (USNC-URSI) in 2016 and 2017. He has been a Phi Kappa Phi member since 2015.

ALEXANDER HOVSEPIAN (Student Member, IEEE) received the B.S.E.E. degree from the University of Washington, Seattle, WA, USA, in 2015, and the M.S. degree from Ohio State University, Columbus, OH, USA, in 2017. He is currently pursuing the Ph.D. degree with Florida International University, Miami, FL, USA. His research interests include high isolation antennas for simultaneous transmit and receive, ultra wideband arrays, and PCB antennas. He was the recipient of the Honorable Mention Award in the Student Paper Competition at APS/URSI in 2018 and 2020.

ALEXANDER D. JOHNSON (Student Member, IEEE) received the B.S. degree in electrical engineering from Western New England University, Springfield, MA, USA, in 2016, the M.S. degree in electrical engineering from Ohio State University, Columbus, OH, USA, in 2017, and the Ph.D. degree in electrical and computer engineering from Florida International University (FIU), Miami, FL, USA, in 2019.

He is currently a part-time Principal Scientist with BAE Systems, Nashua, NH, USA, and has been a Research Assistant Professor with FIU, since August 2019. His research interests include novel materials, textile electronics, wideband array apertures, mm-wave phased arrays, and simultaneous transmit and receive systems. He was a NASA Research Announcement Fellowship Award recipient in 2018. He also received an Honorable Mention in the Student Paper Competition at the 2019 IEEE Antenna and Propagation Symposium (AP-S/URSI), and the Student Fellowship Travel Grant Award at the U.S. National Committee for the International Union of Radio Science (USNC-URSI) in 2017 and 2018.

TOSHIFUMI NAKATANI (Senior Member, IEEE) received the B.E. and M.E. degrees in electrical engineering from Kyoto University, Japan, in 1994 and 1996, respectively, and the Ph.D. degree in electrical engineering from the University of California at San Diego (UCSD), La Jolla, CA, USA, in 2013.

In 1996, he joined the Matsushita Electric Industrial Company Ltd. (currently, Panasonic Corporation), Osaka, Japan, where he was mainly involved with the development of RFIC for cell phone handset using SiGe BiCMOS technology. In 2008, he was with UCSD as a Visiting Scholar, and since 2010, he has been with the Panasonic Corporation of North America, Cupertino. In both places, he is involved in the development of digitally-assisted power amplifier for handset applications. From 2011 to 2012, he was engaged in mm-wave IC project with Panasonic Corporation, Yokohama, Japan. Since 2013, he has been with MaXentric Technologies LLC, where he is involved in multiple small business innovative research programs for developing high-frequency circuits and wireless systems, such as envelope tracking power amplifiers, millimeter-wave GaN power amplifiers, phased array systems and in-band full duplex transceiver systems. He has published over 50 papers, received 34 U.S. patents. His research interests include development of microwave and mm-wave circuits and wireless transceiver systems for communication and satellite applications.

Dr. Nakatani is a member of the Institute of Electronics, Information and Communication Engineers.

ELIAS A. ALWAN (Member, IEEE) was born in Aitou, Lebanon, in 1984. He received the B.E. degree (*summa cum laude*) in computer and communication engineering from Notre Dame University–Louaize, Zouk Mosbeh, Lebanon, in 2007, the M.E. degree in electrical engineering from the American University of Beirut, Beirut, Lebanon, in 2009, and the Ph.D. degree in electrical and computer engineering from Ohio State University (OSU), Columbus, OH, USA, in 2014. He is an Assistant Professor with the Electrical and Computer Engineering Department, Florida International University. He was a Senior Research Associate with the ElectroScience Laboratory, OSU, from 2015 to 2017. His research is in the areas of antennas and radio frequency systems with particular focus on ultra-wideband (UWB) communication systems, including UWB arrays, reduced hardware and power-efficient communication back-ends, and millimeter-wave technologies for 5G applications. He is the recipient of the 2020 NSF CAREER Award. He has been a Phi Kappa Phi member since 2010.

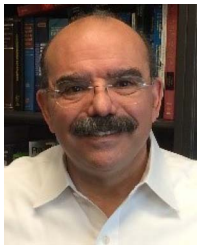

JOHN L. VOLAKIS (Fellow, IEEE) was born in May 13, 1956, in Chios, Greece, and immigrated to the USA, in 1973. He received the B.E. degree (*summa cum laude*) from Youngstown State University, Youngstown, OH, USA, in 1978, the M.Sc. and Ph.D. degrees from Ohio State University, Columbus, OH, in 1979 and 1982, respectively.

He started his career with Rockwell International (currently, Boeing) from 1982 to 1984. In 1984, he was appointed Assistant Professor with the University of Michigan, Ann Arbor, MI, USA, becoming a Full Professor in 1994. He also served as the Director of the Radiation Laboratory from 1998 to 2000. From January 2003 to August 2017, he was the Roy and Lois Chope Chair Professor of engineering with Ohio State University and served as the Director of the ElectroScience Laboratory from 2003 to 2016. Since August 2017, he has been the Dean of the College of Engineering and Computing and a Professor in the electrical and computer engineering with Florida International University. His publications include eight books, 430 journal papers, nearly 900 conference papers, 29 book chapters and 25 patents/disclosures. His coauthored books are *Approximate Boundary Conditions in Electromagnetics* (1995), *Finite Element Methods for Electromagnetics* (1998), *Antenna Engineering Handbook*, 4th ed., (2007), *Small Antennas* (2010), and *Integral Equation Methods for Electromagnetics* (2011). Over the years, he carried out research in antennas, wireless communications and propagation, computational methods, electromagnetic compatibility and interference, design optimization, RF materials, multiphysics engineering, millimeter waves, terahertz, and medical sensing. He has graduated/mentored 95 doctoral students/postdoctorals with 43 of them receiving best paper awards at conferences. Among his awards are the University of Michigan College of Engineering Research Excellence Award in 1993, the Scott Award from the Ohio State University College of Engineering for Outstanding Academic Achievement in 2011, the IEEE AP Society C.-T. Tai Teaching Excellence Award in 2011, the IEEE Henning Mentoring Award in 2013, the IEEE Antennas and Propagation Distinguished Achievement Award in 2014, the Ohio State University Distinguished Scholar Award in 2016, and the Ohio State University ElectroScience George Sinclair Award in 2017, and the URSI Booker Gold Medal in 2020. He was listed by ISI as among the top 250 most referenced authors in 2004, and is a Fellow of ACES and URSI. His service to professional societies include President of the IEEE Antennas and Propagation Society in 2004, Chair of USNC/URSI Commission B from 2015 to 2017, twice the General Chair of the IEEE Antennas and Propagation Symposium, IEEE APS Distinguished Lecturer, the IEEE APS Fellows Committee Chair, a IEEE-Wide Fellows committee member and an associate editor of several journals.